Hindawi
Mathematical Problems in Engineering
Volume 2022, Article ID 4730870, 9 pages
https://doi.org/10.1155/2022/4730870

Research Article

Load Frequency Control for Interconnected Multi-area Power Systems with the Semi-Markov Jumping Parameter and Actuator Failure

Yanjun Jiang,[1] Jinfeng Wang ,[1] Zeyang Bai,[2] Zhengmou Ren,[1] Xiaochen Sun,[1] and Guangliang Yu[1]

[1]*State Grid Shaanxi Electric Power Economic Technology Research Institute, Xi'an, Shaanxi 710065, China*
[2]*State Grid Shaanxi Electric Power Company Limited, Xi'an, Shaanxi 710048, China*

Correspondence should be addressed to Jinfeng Wang; dk.618@stu.xjtu.edu.cn

Received 18 May 2022; Revised 8 June 2022; Accepted 14 June 2022; Published 1 July 2022

Academic Editor: Yong Chen

In this study, we study the load frequency control (LFC) problem for interconnected multiarea power systems (IMAPSs) with quantization and actuator failure. To effectively reduce the amount of data in the channel, input signals will be quantized before being transmitted from a controller to a system through the digital communication channel. To reveal the asynchronous phenomenon between the original plant and LFC with actuator failure, a hidden semi-Markov model is formulated. In addition, the stability of the jump system under network attack is discussed. On the basis of the Lyapunov theory, sufficient conditions are derived to ensure the stochastic stability of IMAPSs. Finally, the validity of the theoretical results is tested via a simulation example.

1. Introduction

The power system is a complex nonlinear system, which has developed into a multiregional interconnected power system (PS) since the Industrial Revolution. To deal with the low-frequency little oscillations of interconnected PSs, the LFC was proposed in [1], which has been effectively applied to PSs [2–4]. According to the LFC technique, the frequency can be adjusted at a desired level, which guarantees the stability of entire PSs. Over the past few decades, researchers have proposed a number of techniques concerning with LFC, such as use of the integral control law [5], PI case [6], and PID case [7]. These approaches have been verified to improve the control performance of interconnected PSs [8, 9].

In practical applications, the dynamic systems may undergo sudden changes in their parameters or structures due to component failures, sudden environmental changes, etc. In this case, Markov chains are widely adopted to model the variations in PS states. In [10], the Markov chain was employed to describe the random mutations of the discrete-time PS. In [11], the uncertain Markov chain was applied for the decentralized control of the PS. However, in most existing literature concerning Markov PSs, the residence time of Markov processes obeys a memory-free random distribution, in which the probability of the transition rate is time-independent. As signified in [12–14], compared with the conventional Markov chain, the semi-Markov chain is more general in approximating practical dynamics owing to its time-varying transition rate. Consequently, it is meaningful to study the LFC problem for PSs with semi-Markov jumping parameters, the so-called semi-Markov PSs. To the best of our knowledge, quite a few theoretical results have been applied to semi-Markov PSs due to their inherent difficulty, and this motivates this article.

In reality, the signal is communicated through a limited bandwidth network [13, 15, 16]. Note that massive signals are transmitted via the limited network, which may lead to channel congestion, thus reducing the system performance. To overcome this shortcoming, we quantify the control inputs, in which quantization stands for the process of mapping the continuous values of a signal to a limited

number of discrete values [17, 18]. By means of quantization, the amount of data in the channel and load of the channel can be effectively reduced. The quantizers can be roughly categorized into linear quantizers [19], and logarithm quantizers [20, 21]. The problem of stabilizing a continuous-time switched system affected by the time-varying delay and data quantization has been addressed in [22]. In the quantitative input multiarea, however, results of the power system are very few; in order to fill the gap, this article takes into account the interconnected more regional power system with quantitative input, and the quantification method is used as the basis of the design, making the obtained quantitative instruments with the crudest density and further reducing the burden of transmission. We would like to mention that, in practice, capturing system information is a tricky task. Therefore, the asynchrony between the system mode and the controller mode cannot be omitted. Nevertheless, the asynchronous control of the semi-Markov IMAPS has not been researched thoroughly, which partially motivates the current work.

Motivated by the above considerations, this work considers the LFC problem of the IMAPS subject to quantization input. Different from the existing homogeneous Markov IMAPS, the semi-Markov chain is employed to describe the dynamic behavior of the IMAPS. Aiming to describe the asynchronous phenomenon between the original plant and LFC, the hidden semi-Markov model is formulated. By resorting to the Lyapunov theory, sufficient conditions are derived to ensure the stochastic stability of the resulting dynamic. In the end, one numerical example is inferred to show the correctness of the proposed method. The general structure is rendered as follows: the second section describes the asynchronous LFC of the semi-Markov PS with quantization form. In section 3, sufficient conditions of random stability are given. A numerical example is given in section 4.

Notations: diag$\{*\}$ means a block-diagonal matrix; $He\{R\} = R + R^{\top}$; $P > 0$ means P is positive definite; Pr$\{*\}$ implies occurrence probability; $\varepsilon\{*\}$ indicates the mathematical expectation; $\|*\|$ signifies the Euclidean vector norm. $\mathfrak{I}$ signifies the identity matrix; $A^{\top}$ and A^{-1} stand for the transpose and inverse matrix, respectively.

2. Problem Formulations

2.1. System Model. In this study, the dynamic model of the multiarea LFC is described as follows:

$$\begin{cases} \dot{x}(t) = A(r(t))x(t) + H(r(t))\Delta P_L(t) + B(r(t))u(t), \\ y(t) = C(r(t))x(t), \end{cases} \tag{1}$$

where $x_i(t) \in \mathbb{R}^5$, $y_i(t) \in \mathbb{R}^2$, $u_i(t) \in \mathbb{R}$, and $\Delta P_L^i(t) \in \mathscr{L}_2[0, \infty)$ represent the state, the output, the control input, and the disturbance, respectively, and

$$y_i(t) = \left[\mathrm{ACE}_i \quad \int_0^t \mathrm{ACE}_i(s)\mathrm{d}s \right]^{\top},$$

$$y(t) = \left[y_1(t) y_2(t) \cdots y_N(t) \right]^{\top},$$

$$u(t) = \left[u_1(1) u_2(t) \cdots u_N(t) \right]^{\top},$$

$$\Delta P_L(t) = \left[\Delta P_L^1(t) \Delta P_L^2(t) \cdots \Delta P_L^N(t) \right]^{\top},$$

$$x_i(t) = \left[\Delta f_i(t), \Delta P_m^i(t), \Delta Y_i(t), \Delta P_{tie}^i(t), \int_0^t ACE_i(s)\mathrm{d}s \right] \top,$$

$$x(t) = \left[x_1(t) x_2(t) \cdots x_N(t) \right]^{\top},$$

$$B_i(r(t)) = \left[0 \;\; 0 \;\; \frac{1}{T_g(i)(r(t))} \;\; 0 \;\; 0 \right]^{\top},$$

$$B(r(t)) = \mathrm{diag}\{B_1(r(t)) B_2(r(t)) \cdots B_N(r(t))\},$$

$$H_i(r(t)) = \left[-\frac{1}{M_i(r(t))} \;\; 0 \;\; 0 \;\; 0 \;\; 0 \right]^{\top},$$

$$H(r(t)) = \mathrm{diag}\{H_1(r(t)) H_2(r(t)) \cdots H_N(r(t))\}$$

$$C_i(r(t)) = \begin{pmatrix} \beta_i(r(t)) & 0 & 0 & 1 & 0 \\ 0 & 0 & 0 & 0 & 1 \end{pmatrix},$$

$$C(r(t)) = \mathrm{diag}\{C_1(r(t)) C_2(r(t)) \cdots C_N(r(t))\},$$

$$A_{ii}(r(t)) = \begin{pmatrix} -\frac{D_i(r(t))}{M_i(r(t))} & \frac{1}{D_i(r(t))} & 0 & -\frac{1}{D_i(r(t))} & 0 \\ 0 & -\frac{1}{T_t^i(r(t))} & \frac{1}{T_t^i(r(t))} & 0 & 0 \\ -\frac{1}{R_i(r(t))T_g^i(r(t))} & 0 & -\frac{1}{T_g^i(r(t))} & 0 & 0 \\ \sum_{j=1, j\neq i}^{N} 2\pi T_{ij}(r(t)) & 0 & 0 & 0 & 0 \\ \beta_i(r(t)) & 0 & 1 & 0 & 0 \end{pmatrix}. \tag{2}$$

$A_{ij} = [a_{ls}]_{l,s=1}^{5}$ with $a_{51} = -2\pi T_{ij}$, $a_{ls} = 0$, and $A = [A_{ij}]_{j,i=1}^{N}$. Each ACE signal is described as a linear combination of the tie-line power exchange and frequency deviation, i.e., $\mathrm{ACE}_i = \beta_i(r(t))\Delta f_i(t) + P_{\mathrm{tie}}^i(t)$, where $\Delta P_{\mathrm{tie}}^i$ refers to the net exchange of the tie-line power. The nomenclature of other parameters is shown in Table 1.

In view of the uncertain fault time of the power system, the semi-Markov process $\{r(t)\}_{t\geq 0} \in \mathcal{S} = \{1, 2, \ldots, S\}$ is adopted. For all $k \in \mathbb{N}$,

$$\begin{aligned} &R_k \text{ the Markov chain} \\ &T_k \text{the sojourn time, i.e., } T_k = t_k - t_{k-1} \\ &G_p \text{ the probability distribution function} \\ &\chi_p \text{ the Markov chain.} \end{aligned} \tag{3}$$

Then, $\{(R_k, r_k)\}$ is said to be a renewal process if $r(t) = R_N(t)$ where $N(t) = \sup\{k\colon t \geq t_k\}$ with

$$\Pr\{R_{k+1} = q | R_k = p\} = \begin{cases} \Pi_{pq}, & p \neq q, \\ 0, & p = q. \end{cases} \tag{4}$$

Meanwhile, the probability distribution function G_p can be described as follow:

$$G_p(h) = \Pr\{T_{k+1} < h | r(t_k) = p\}. \tag{5}$$

According to the aforementioned observation, we have

$$\begin{aligned} \Pr\{r(t+\delta) = q | r(t) = p\} &= \begin{cases} \Pr\{T_{k+1} \leq h + \delta, R_{k+1} = q | T_{k+1} > h, R_k = p\}, & p \neq q, \\ \Pr\{T_{k+1} > h + \delta, R_{k+1} = q | T_{k+1} > h, R_k = p\}, & p = q. \end{cases} \\ &= \begin{cases} \pi_{pq}(h)\delta + o(\delta), & p \neq q, \\ 1 + \pi_{pq}(h)\delta + o(\delta), & p = q. \end{cases} \end{aligned} \tag{6}$$

Hence, by simple calculation, the transition rate matrix can be defined by $\Psi(h) = [\pi_{pq}^h]_{S\times S}$, where

$$\begin{aligned} \pi_{pq}(h) &= \lim_{\delta \longrightarrow 0} \frac{\Pr\{r(t+\delta) = q | r(t) = p\}}{\delta} \\ &= \Pi_{pq} \frac{\chi_p(h)}{1 - G_p(h)}, \quad p \neq q, \end{aligned} \tag{7}$$

and $\pi_{pp}(h) = -\sum_{q=1, q\neq p}^{S} \pi_{pq}(h) < 0$.

2.2. Asynchronous Control Input with Quantized. As exhibited in Figure 1, the control input $u(t)$ is required to be quantized before sending it to the power system. Inspired by this fact, the logarithmic quantizer can be described as follows:

$$\mathfrak{q}(u(t)) = [\mathfrak{q}_1(u_1(t))\mathfrak{q}_2(u_2(t)) \cdots \mathfrak{q}_\iota(u_\iota(t))], \tag{8}$$

where the wth subquantizer $\mathfrak{q}_w(\cdot)$ satisfying $\mathfrak{q}_w(u_w(t)) = -\mathfrak{q}_w(-u_w(t))$, $w = 1, 2, \ldots, \iota$. The set of the logarithmic quantization level can be described as

$$\begin{aligned} \mathbb{U}_w = \{ &\pm \theta_n^w \colon \pm \theta_n^w = \rangle_w^n \theta_0^w, \\ &n = \pm 1 \pm 2, \cdots\} \cup \{\pm \theta_0^w\} \cup \{0\}, \end{aligned} \tag{9}$$

where $0 < \varrho_w^n < 1$ and $\theta_0^w > 0$ on behalf of the quantizer density and the initial quantization, respectively .And $\lambda_\omega = 1 - \varrho_w / 1 + \varrho_w$. Then, we define the subquantizer $\mathfrak{q}_\omega(u_\omega(t))$ as

Table 1: The physical meaning of parameters.

Parameters	Nomenclature
$\Delta f_i(t)$	Frequency deviation
$\Delta P_m^i(t)$	Mechanical power output increment
$\Delta Y_i(t)$	Valve position of turbine
$D_i(r(t))$	Mode-dependent damping coefficient
$T_t^i(r(t))$	Turbine time constant
$T_g^i(r(t))$	Governor time constant
$\beta_i(r(t))$	Frequency bias
$T_{ij}(r(t))$	Coefficient between the i-th and j-th area

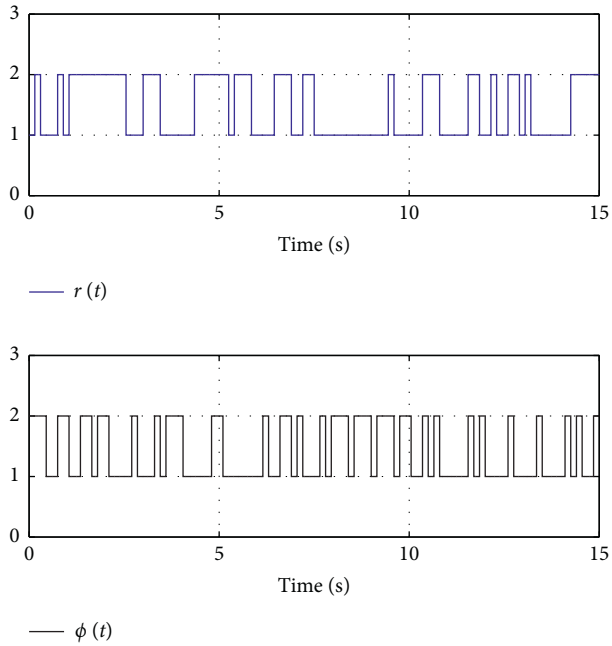

Figure 1: The evolution of modes $r(t)$ and $\varphi(t)$.

$$\mathfrak{q}_\omega(u_\omega(t)) = \begin{cases} \theta_n^\omega, & \text{if} \quad \dfrac{\theta_n^\omega}{1+\lambda_\omega} < u_\omega(t) < \dfrac{\theta_n^\omega}{1-\lambda_\omega}, \\ 0, & \text{if} \quad u_\omega(t) = 0, \\ -\mathfrak{q}_\omega(-u_\omega(t)), & \text{if} \quad u_\omega(t) < 0. \end{cases} \tag{10}$$

Then, we have that

$$\mathfrak{q}(u(t)) = u(t), \tag{11}$$

where $\Lambda = \text{diag}\{\Lambda_1, \Lambda_2, \ldots, \Lambda_\iota\}$, $\Lambda_w^\top \Lambda_w \le \mathfrak{F}$.

In this work, the i-th control area of an asynchronous PI controller is given by

$$\begin{aligned} u_i(t, \varphi(t)) &= K_{P\varphi(t)}^i ACE_i(t) + K_{I\varphi(t)}^i \int_0^t \text{ACE}_i(s)\text{d}s \\ &= K_{\varphi(t)}^i y_i(t), \end{aligned} \tag{12}$$

where $K_{P\varphi(t)}^i$, and $K_{I\varphi(t)}^i$ are the i -th proportional and integral gains, respectively, and $K_{\varphi(t)}^i = [K_{P\varphi(t)}^i \, K_{I\varphi(t)}^i]$. The variable $\varphi(t)$ that refers to the Markov chain belongs to the space $\mathscr{M} = \{1, 2, \ldots, M\}$, whose conditional probability matrix is inferred $\Gamma = [\rho_{pm}]_{S\times M}$ with

$$\Pr\{\varphi(t) = m | r(t) = p\} = \rho_{pm}, \tag{13}$$

with $\sum_{m\in\mathscr{M}} \rho_{pm} = 1$. According to equations (11) and (12), the control signal $u_i(t, \varphi(t))$ can be devised as follows:

$$u_i(t, \varphi(t)) = a_i(t)\left(\mathfrak{F}_i + \Lambda_i\right) K_{\varphi(t)}^i y_i(t), \tag{14}$$

where $a_i(t) \in \{0, 1\}$, and $\varepsilon\{a_i(t)\} = \overline{a}_i$.

2.3. Model Transformation. Let $r(t) = p$ and $\varphi(t) = m$, substituting equations (14) into (1), the closed-loop IMAPS is formulated as follows:

$$\begin{cases} \dot{x}_i(t) = A_p^{ii}x_i(t) + \sum_{j=1,j\neq i}^{N} A_p^{ij}x_j(t) + \overline{a}_i B_p^i(\mathfrak{F}_i + \Lambda_i)K_{pm}^i C_p^i x_i(t) + H_p^i \Delta P_L^i(t), \\ y_i(t) = C_p^i x_i(t). \end{cases} \tag{15}$$

For analysis convenience, based on the compatible matrix $\widehat{B}_p^i$, we can obtain a full rank matrix $\overline{B}_p^i = [B_p^i \ \widehat{B}_p^i]$. We define $\mathfrak{X}_i(t) = (\overline{B}_p^i)^{-1}x_i(t)$, we have that

$$\begin{cases} \dot{\mathfrak{X}}_i(t) = \overline{A}_p^{ii}\mathfrak{X}_i(t) + \sum_{j=1,j\neq i}^{N} \overline{A}_p^{ij}\mathfrak{X}_j(t) + \overline{a}_i(\mathfrak{F}_i + \Lambda_i)\overline{K}_m^i C_p^i \mathfrak{X}_i(t) + \overline{H}_p^i \Delta P_L^i(t), \\ y_i(t) = \overline{C}_p^i \mathfrak{X}_i(t), \end{cases} \tag{16}$$

where $\overline{A}_p^{ij} = (\overline{B}_p^i)^{-1}A_p^{ij}\overline{B}_p^i$, $\overline{K}_m = [(K_m^i)^\top \quad 0]\top$, $\overline{C}_p^i = C_p^i\overline{B}_p^i$, and $\overline{H}_p^i = (\overline{B}_p^i)^{-1}H_p^i$. It is worth noting that linear transformation $\overline{B}_p^i$ is invertible. Thus, the overall IMAPS can be inferred as

$$\begin{cases} \dot{\mathfrak{X}}(t) = \overline{A}_p\mathfrak{X}(t) + \overline{a}(\mathfrak{F} + \Lambda)\overline{K}_m\overline{C}_p\mathfrak{X}(t) + \overline{H}_p\Delta P_L(t), \\ y(t) = \overline{C}_p\mathfrak{X}(t), \overline{C}_p\mathfrak{X}(t), \end{cases} \tag{17}$$

where $\overline{a} = \mathrm{diag}_N\{\overline{a}_i\}$, $\mathfrak{F} + \Lambda = \mathrm{diag}_N\{(\mathfrak{F}_i + \Lambda_i)\}$, $\overline{C}_p = \mathrm{diag}_N\{\overline{C}_p^i\}$, $\overline{H}_p^i = \mathrm{diag}_N\{\overline{H}_p^i\}$, and

$$\overline{A}_p = \begin{bmatrix} \overline{A}_p^{11} & \overline{A}_p^{12} & \cdots & \overline{A}_p^{1N} \\ \overline{A}_p^{21} & \overline{A}_p^{22} & \cdots & \overline{A}_p^{2N} \\ \vdots & \vdots & \ddots & \vdots \\ \overline{A}_p^{N1} & \overline{A}_p^{N2} & \cdots & \overline{A}_p^{NN} \end{bmatrix}. \tag{18}$$

Definition 1. ([23]) The interconnected power system with $\Delta P_L(t) = 0$ is called stochastic stability if the following equation holds:

$$\varepsilon\left\{\int_0^\infty \|\mathfrak{X}(t)\|^2 \mathrm{d}t | r(t_0), \varphi(t_0)\right\} < \infty. \tag{19}$$

Under the zero initial condition, the system with $\Delta P_L(t) \in \mathscr{L}_2[0,\infty)$ and $\gamma > 0$, the H_∞ performance index is satisfied:

$$\varepsilon\left\{\int_0^\infty y^T(t)y(t) - \gamma^2 P_L^T(t)P_L(t)\right\} < 0. \tag{20}$$

Lemma 1. *([21]) For the given matrix Ω_1 and matrices Ω_2 and Ω_3 with appropriate dimensions, if inequality $\Omega_1 + He\{\Omega_2\Lambda\Omega_3\} < 0$ holds for all $\|\Lambda\| \le \mathfrak{F}$, for any scalar s_1, such that $\Omega_1 + s_1\Omega_3^\top\Omega_3 + s_1^{-1}\Omega_2^\top\Omega_2 < 0$.*

3. Main Results

Theorem 1. *For given scalars $\gamma > 0$ and $\eta > 0$ and the matrix M_p, the IMAPS is stochastic stability with preset performance, such that*

$$\overline{\Xi}_{pm} = \begin{bmatrix} \Xi_{pm}^{11} + \overline{C}_p^\top\overline{C}_p & * & * \\ \Xi_{pm}^{21} & -He\{\eta M^\top\} & * \\ \overline{H}_p^\top M^\top & \eta\overline{H}_p^\top M^\top & -\gamma^2 \end{bmatrix} < 0, \tag{21}$$

where

$$\begin{aligned} \Xi_{pm}^{11} &= \sum_{q=1}^{S}\overline{\Pi}P_q + \sum_{m=1}^{M}\rho_{pm}He\left\{M^\top\left(\overline{A}_p + \overline{a}(\mathfrak{F} + \Lambda)\overline{K}_m\overline{C}_p\right)\right\}, \\ \Xi_{pm}^{21} &= -M + P_p^\top + \sum_{m=1}^{M}\rho_{pm}\eta M^\top\left(\overline{A}_p + \overline{a}(\mathfrak{F} + \Lambda)\overline{K}_m\overline{C}_p\right), \\ \overline{\Pi}_{pq} &= \varepsilon\{\pi_{pq}(h)\} = \int_0^\infty \pi_{pq}(h)\chi_p(h)\mathrm{d}h. \end{aligned} \tag{22}$$

Proof. Establish the semi-Markov-based Lyapunov function as follows:

$$V(\mathfrak{X}(T), r(t), \varphi(t)) = \mathfrak{X}^\top(t)P_{r(t)}\mathfrak{X}(t). \tag{23}$$

It follows that

$$\varepsilon\{\mathscr{L}V(\mathfrak{X}(t),r(t),\varphi(t))\} = \lim_{\delta\longrightarrow 0} \frac{1}{\delta}\left\{\varepsilon\left\{\sum_{q\neq p}\pi_{pq}(h)\delta\mathfrak{X}^{\top}(t+\delta)P_q\mathfrak{X}(t+\delta)+\left(1+\pi_{pp}(h)\delta\right)\mathfrak{X}^{\top}(t+\delta)P_p\mathfrak{X}(t+\delta)\right\}+\mathfrak{X}^{\top}(t)P_p\mathfrak{X}(t)\right] = \mathfrak{X}^{\top}(t)\left(\sum_{q=1}^{S}\overline{\Pi}_{pq}P_q\right)\mathfrak{X}(t)+He\left\{\dot{\mathfrak{X}}^{\top}(t)P_p\mathfrak{X}^{\top}(t)\right\}. \tag{24}$$

On the basis of equation (17), for any proper matrix M, such that

$$0 = 2\left[\mathfrak{X}^{\top}(t)M^{\top}+\eta\dot{\mathfrak{X}}(t)M^{\top}\right]\times\left[-\dot{\mathfrak{X}}(t)+\overline{A}_p\mathfrak{X}(t)+\overline{a}(\mathfrak{F}+\Lambda)\overline{K}_m\overline{C}_p\mathfrak{X}(t)+\overline{H}_p\Delta P_L(t)\right]. \tag{25}$$

It follows from equations (24) and (25) that

$$\begin{aligned}&\varepsilon\{\mathscr{L}V(\mathfrak{X}(t),r(t),\varphi(t))\}\\&\quad=\mathfrak{X}^{\top}(t)\left(\sum_{q=1}^{S}\overline{\Pi}_{pq}P_q\right)\mathfrak{X}(t)+He\left\{\dot{\mathfrak{X}}^{\top}(t)P_p\mathfrak{X}^{\top}(t)\right\}\\&\qquad+2\left[\mathfrak{X}^{\top}(t)M^{\top}+\eta\dot{\mathfrak{X}}(t)M^{\top}\right]\times\left[-\dot{\mathfrak{X}}(t)+\overline{A}_p\mathfrak{X}(t)+\overline{a}(\mathfrak{F}+\Lambda)\overline{K}_m\overline{C}_p\mathfrak{X}(t)+\overline{H}_p\Delta P_L(t)\right]\\&\quad=\zeta^{\top}(t)\Xi_{pm}\zeta(t),\end{aligned} \tag{26}$$

where $\zeta^{\top}(t)=[\xi^{\top}(t)\quad \Delta P^{\top}(t)]$, $\xi^{\top}(t)=[\mathfrak{X}^{\top}(t)\quad \dot{\mathfrak{X}}^{\top}(t)]$ $\overline{\Pi}_{pq}=\varepsilon\{\pi_{pq}(h)\}=\int_0^{\infty}\pi_{pq}(h)\chi_p(h)dh$ and

$$\Xi_{pm}=\begin{bmatrix}\Xi_{pm}^{11} & * & *\\ \Xi_{pm}^{21} & -He\{\eta M^{\top}\} & *\\ \overline{H}_p^{\top}M^{\top} & \eta\overline{H}_p^{\top}M^{\top} & 0\end{bmatrix}. \tag{27}$$

In case of $\Delta P_L(t)=0$, we have $\varepsilon\{\mathscr{L}V(\mathfrak{X}(t),r(t),\varphi(t))\}\le\xi^{\top}(t)\Xi_{pm}^{1}\xi^{\top}(t)$, by equation (21), we have $\Xi_{pm}^{1}<0$, when $\Xi_{pm}^{1}=\begin{bmatrix}\Xi_{pm}^{11} & *\\ \Xi_{pm}^{21} & -He\{\eta M^{\top}\}\end{bmatrix}$, $\Xi_{pm}^{11}=\sum_{q=1}^{S}\overline{\Pi}P_q+\sum_{m=1}^{M}\rho_{pm}He\{M^{\top}(\overline{A}_p+\overline{a}(\mathfrak{F}+\Lambda)\overline{K}_m\overline{C}_p)\}$, $\Xi_{pm}^{21}=-M+P_p^{\top}+\sum_{m=1}^{M}\rho_{pm}\eta M^{\top}(\overline{A}_p+\overline{a}(\mathfrak{F}+\Lambda)\overline{K}_m\overline{C}_p)$. Subsequently, we have

$$\begin{aligned}&\varepsilon\{\mathscr{L}V(\mathfrak{X}(t),r(t),\varphi(t))\}\\&\quad\le-\lambda\varepsilon\left\{\|\mathfrak{X}(t)\|^2\mid\mathfrak{X}(t_0),r(t_0),\varphi(t_0)\right\},\end{aligned} \tag{28}$$

where $\lambda=\lambda_{\min}(-\Xi_{pm}^{1})$, we can further have

$$\begin{aligned}&\varepsilon\left\{\int_0^{\infty}\|\mathfrak{X}(t)\|^2|\mathfrak{X}(t_0),r(t_0),\varphi(t_0)\right\}\\&\quad\le\frac{1}{\lambda}V(\mathfrak{X}(t_0),r(t_0),\varphi(t_0))<\infty.\end{aligned} \tag{29}$$

Furthermore, for $\Delta P_L(t)\neq 0$, according to equation (24), it yields

$$\mathscr{L}V+y^{\top}(t)y(t)-\gamma^2\Delta P_L^{\top}(t)\Delta P_L(t)\le\zeta^{\top}(t)\overline{\Xi}_{pm}\zeta(t). \tag{30}$$

Note that $\overline{\Xi}_{pm}<0$, from which one can obtain

$$\int_0^{\infty}\left(\mathscr{L}V+z^{\top}(t)z(t)-\gamma^2\Delta P_L^{\top}(t)\Delta P_L(t)\right)dt<0, \tag{31}$$

which indicates

$$\int_0^{\infty}\left(z^{\top}(t)z(t)-\gamma^2\Delta P_L^{\top}(t)\Delta P_L(t)\right)dt<0, \tag{32}$$

this completes the proof. □

Theorem 2. *For given scalars $\gamma>0$, $\eta>0$, and $s_1>0$, system equation (13) is stochastic stability with the preset H_∞ performance index γ, if there exist matrices M and $\overline{K}_m$, such that*

$$\begin{bmatrix} \overline{\Xi}_{pm}^{11} & * & * & * & * & * & * \\ \overline{\Xi}_{pm}^{21} & -He\{\eta M^{\top}\} & * & * & * & * & * \\ \overline{H}_p^{\top} M^{\top} & \eta \overline{H}_p^{\top} M^{\top} & -\gamma^2 \mathfrak{I} & * & * & * & * \\ \overline{C}_p & 0 & 0 & -\mathfrak{I} & * & * & * \\ \theta_p^{\top} & 0 & 0 & 0 & \theta_p^{11} & * & * \\ \left(\theta_p^{111}\right)^{\top} & \eta\left(\theta_p^{111}\right)^{\top} & 0 & 0 & 0 & -He\{\widehat{a}\overline{s}_1\} & * \\ M^{\top} & \eta M^{\top} & 0 & 0 & 0 & 0 & -He\{\widehat{a}s_1\} \end{bmatrix} < 0, \tag{33}$$

where $\overline{s}_1 = s_1^{-1}$, $\widehat{a} = \eta \overline{a}^{-1}$

$$\begin{aligned} \overline{\Xi}_{pm}^{11} &= \overline{\Pi}_{pp} P_p + He\left\{M^{\top} \overline{A}_p\right\} + \sum_{m=1}^{M} \rho_{pm} He\left\{\overline{a} Y \mathscr{K}_m \overline{C}_p\right\}, \\ \overline{\Xi}_{pm}^{21} &= -M + P_p^{\top} + \sum_{m=1}^{M} \rho_{pm} \overline{a} \eta Y \mathscr{K}_m \overline{C}_p \\ \theta_p^{11} &= -\mathrm{diag}\left\{P_1 P_2 \cdots P_{p-1} P_{p+1} \cdots P_S\right\}, \\ \theta_p^{111} &= \left[\sqrt{\rho_{p1}} \overline{C}^{\top} \overline{K}_1^{\top} \sqrt{\rho_{p2}} \overline{C}^{\top} \overline{K}_2^{\top} \cdots \sqrt{\rho_{pM}} \overline{C}^{\top} \overline{K}_M^{\top}\right] \\ \theta_p &= \left[\sqrt{\overline{\Pi}_{p1}} P_1 \sqrt{\overline{\Pi}_{p2}} P_2 \cdots \sqrt{\overline{\Pi}_{p(p-1)}} P_{p-1} \sqrt{\overline{\Pi}_{p(p+1)}} P_{p+1} \cdots \sqrt{\overline{\Pi}_{pS}} P_S\right], \\ Y &= \mathrm{diag}\{Y_1, Y_2, \ldots, Y_N\}, \quad Y_i = \mathrm{diag}\left\{\mathfrak{I}_p, 0\right\}. \end{aligned} \tag{34}$$

Furthermore, controller gain matrices are given by $\overline{K}_m = (M^{\top})^{-1} Y \mathscr{K}_m$.

Proof. Let $Y\mathscr{K}_m = M^{\top}\overline{K}_m$, with the purpose of structure of the matrix $\overline{K}_m$. In detail,

$$\overline{K}_m^i = \left(M_i^{\top}\right)^{-1} Y_i \mathscr{K}_m^i == \begin{bmatrix} M_{1i}^{-1} & 0 \\ 0 & M_{2i}^{-1} \end{bmatrix} \begin{bmatrix} \mathfrak{I}_p & 0 \\ 0 & 0 \end{bmatrix} \mathscr{K}_m^i. \tag{35}$$

According to Lemma 1 and by using the Schur complement in equation (21)(10) the proof is completed. □

4. Numerical Example

In this section, to show the effectiveness of the attached methodology, a numerical example of the 3-area interconnected semi-Markov switching power system is presented. Suppose that the coefficients are selected $T_{12}(r(t)) = 0.2$, $T_{13}(r(t)) = 0.25$, and $T_{23}(r(t)) = 0.12$, $r(t) = 1, 2$. Furthermore, for any $i = 1, 2, 3$, set

$$\widehat{B}_p^i = \begin{bmatrix} 0.001 & 0 & 0 & 0 \\ 0 & 0.001 & 0 & 0 \\ 0 & 0 & 0.001 & 0 \\ 0 & 0 & 0.001 & 0.001 \end{bmatrix}. \tag{36}$$

Let $\overline{a}_i = 0.5$, $\gamma = 7$, $\eta = 0.2$, and $s_1 = 0.4$. Other nominal parameters are listed in Table 2 [3, 24].

Specifically, the transition rate function can be written $\pi_{pq} = \Pi_{pq}(h) k/\epsilon^k h^{k-1}$, and the Weibull distribution density function is given by $\chi_p(h) = k/\epsilon(h/\epsilon)^{k-1} \exp(-(h/\epsilon)^k)$, where k and ϵ indicate the parameters of the shape and scale, respectively. Noting that when $p = 1$, we choose $\epsilon = 1$ and $k = 3$. Otherwise, for $p = 2$, we set $\epsilon = 1$ and $k = 4$. Accordingly, the transition rate matrix can be expressed as

$$\pi_{pq}(h) = \begin{bmatrix} -3h^2 & 3h^2 \\ 4h^3 & -4h^3 \end{bmatrix}. \tag{37}$$

Thus, we have

$$\begin{aligned} \overline{\Pi}_{pq} &= \varepsilon\{\pi(h)\} \\ &= \begin{bmatrix} -2.7082 & 2.7082 \\ 3.6763 & -3.6763 \end{bmatrix}. \end{aligned} \tag{38}$$

In order to better describe the asynchronous phenomenon, the condition probability matrix is set as follows $\Gamma = [0.6\ \ 0.4;\ 0.5\ \ 0.5]$. According to Theorem 2, the asynchronous controller gains can be easily devised. We select the initial state $x_{10} = [0.048\ -0.04\ 0.065\ 0.024\ -0.55]^{\top}$, $x_{20} = [0.045\ -0.09\ 0.015\ 0.022\ -0.46]^{\top}$, $x_{30} = [0.07\ -0.05\ 0.07\ -0.08\ -1.1]^{\top}$, and the load disturbance $\Delta P_L^i = 0.005 \quad \sin(k)$, $(i = 1, 2, 3)$. Added by the

Table 2: Parameters of the IMAPS.

	Mode	$M_i(r(t))$	$D_i(r(t))$	$T_t^i(r(t))$	$T_g^i(r(t))$	$\beta_i(r(t))$	$R_i(r(t))$
Area 1	$r=1$	10	1	0.3	0.1	21	0.05
	$r=2$	10	1.1	0.35	0.15	20.5	0.05
Area 2	$r=1$	12	1	0.4	0.17	21.5	0.05
	$r=2$	10	1.5	0.4	0.1	18	0.05
Area 3	$r=1$	12	1.8	0.35	0.12	21.8	0.05
	$r=2$	12.5	1.25	0.15	0.15	23	0.05

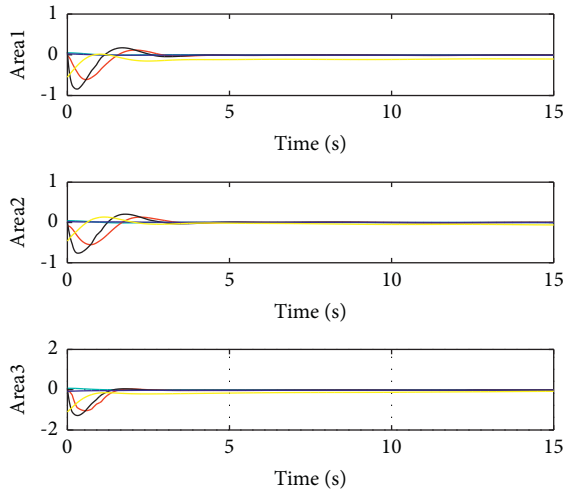

Figure 2: The state trajectories $x_i(t)$ $(i=1,2,3)$.

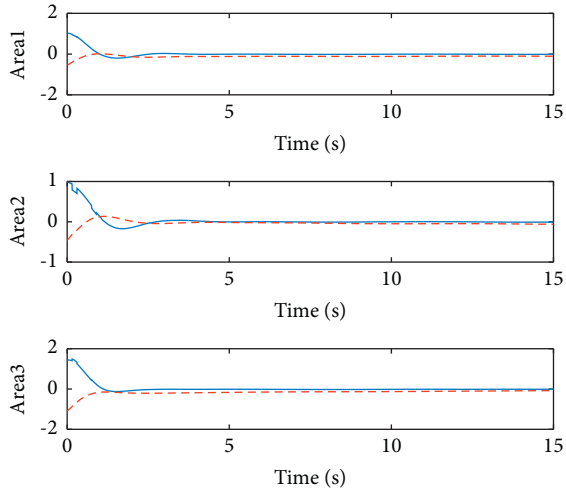

Figure 3: The measured output $y_i(t)$ $(i=1,2,3)$.

above-derived gains, the mode evolution of $r(t)$ and $\varphi(t)$ is shown in Figure 1. The trajectories of the state are plotted in Figure 2. Figure 3 thatdepict the state trajectories and the measured output. These simulation results verify the effectiveness of the proposed method.

5. Conclusions

In this study, the problem of the asynchronous load frequency control problem for semi-Markov interconnected multi-area power systems with the quantization effect has been addressed. In this case, the system under consideration is modeled as the semi-Markov jump system. The merit of this work is to tackle the asynchronous phenomenon between the control and semi-Markov interconnected multi-area power systems. By designing an asynchronous controller with quantized form, the quantized closed-loop system has stochastic stability under the specified performance. At last, the effectiveness of the developed method has been tested by the simulation result.

Data Availability

The data used to support the findings of this study are included in the article.

Conflicts of Interest

The authors declare that they have no conflicts of interest.

References

[1] O. I. Elgerd and C. E. Fosha, "Optimum megawatt-frequency control of multiarea electric energy systems," *IEEE Transactions on Power Apparatus and Systems*, no. 4, pp. 556–563, 1970.

[2] M. Toulabi, M. Shiroei, and A. Ranjbar, "Robust analysis and design of power system load frequency control using the kharitonov's theorem," *International Journal of Electrical Power & Energy Systems*, vol. 55, pp. 51–58, 2014.

[3] H. Zhang, J. Liu, and S. Xu, "Load frequency control of networked power systems via an event-triggered scheme," *IEEE Transactions on Industrial Electronics*, vol. 67, no. 8, pp. 7104–7113, 2019.

[4] H. K. Shaker, H. El Zoghby, M. E. Bahgat, and A. Abdel-Ghany, "Advanced control techniques for an interconnected multi area power system for load frequency control," in *Proceedings of the 2019 21st International Middle East Power Systems Conference (MEPCON)*, pp. 710–715, IEEE, Cario, Egypt, December 2019.

[5] B. Paramasivam and I. Chidambaram, "Design of load-frequency controller using artificial bee colony algorithm for an interconnected power system coordinated with upfc and rfb," *International Journal of computer applications*, vol. 36, no. 5, pp. 1–12, 2011.

[6] Y. Arya, "Automatic generation control of two-area electrical power systems via optimal fuzzy classical controller," *Journal of the Franklin Institute*, vol. 355, no. 5, pp. 2662–2688, 2018.

[7] R. Shankar, A. Kumar, U. Raj, and K. Chatterjee, "Fruit fly algorithm-based automatic generation control of multiarea interconnected power system with facts and ac/dc links in deregulated power environment," *International Transactions*

on Electrical Energy Systems, vol. 29, no. 1, Article ID e2690, 2019.

[8] C. Peng, J. Zhang, and H. Yan, "Adaptive event-triggering H_∞ load frequency control for network-based power systems," *IEEE Transactions on Industrial Electronics*, vol. 65, no. 2, pp. 1685–1694, 2017.

[9] X. Zhao, S. Zou, and Z. Ma, "Decentralized resilient H_∞ load frequency control for cyber-physical power systems under dos attacks," *IEEE/CAA Journal of Automatica Sinica*, vol. 8, no. 11, pp. 1737–1751, 2021.

[10] S. Kuppusamy, Y. H. Joo, and H. S. Kim, "Asynchronous control for discrete-time hidden Markov jump power systems," *IEEE Transactions on Cybernetics*, pp. 1–6, 2021, in press.

[11] V. Ugrinovskii and H. R. Pota, "Decentralized control of power systems via robust control of uncertain Markov jump parameter systems," *International Journal of Control*, vol. 78, no. 9, pp. 662–677, 2005.

[12] M. Perman, A. Senegacnik, and M. Tuma, "Semi-markov models with an application to power-plant reliability analysis," *IEEE Transactions on Reliability*, vol. 46, no. 4, pp. 526–532, 1997.

[13] J. Cheng, L. Xie, J. H. Park, and H. Yan, "Protocol-based output-feedback control for semi-markov jump systems," *IEEE Transactions on Automatic Control*, p. 1, 2022, in press.

[14] L. Xie, J. Cheng, H. Wang, J. Wang, M. Hu, and Z. Zhou, "Memory-based event-triggered asynchronous control for semi-markov switching systems," *Applied Mathematics and Computation*, vol. 415, Article ID 126694, 2022.

[15] J. Cheng, L. Liang, J. H. Park, H. Yan, and K. Li, "A dynamic event-triggered approach to state estimation for switched memristive neural networks with nonhomogeneous sojourn probabilities," *IEEE Transactions on Circuits and Systems I: Regular Papers*, vol. 68, no. 12, pp. 4924–4934, 2021.

[16] J. Cheng, J. H. Park, Z.-G. Wu, and H. Yan, "Ultimate boundedness control for networked singularly perturbed systems with deception attacks: a Markovian communication protocol approach," *IEEE Transactions on Network Science and Engineering*, vol. 9, no. 2, pp. 445–456, 2022.

[17] J. Wang, Z. Xi, and L. Sun, "Dynamic logarithmic vector quantizer design for stochastic continuous time linear systems with state feedback control," *IEEE Access*, vol. 8, pp. 46440–46447, 2020.

[18] J. Cheng, Y. Wang, J. H. Park, J. Cao, and K. Shi, "Static output feedback quantized control for fuzzy Markovian switching singularly perturbed systems with deception attacks," *IEEE Transactions on Fuzzy Systems*, vol. 30, no. 4, pp. 1036–1047, 2022.

[19] H. Saito, I. Umoto, A. Sasou, S. Nakamura, Y. Horio, and T. Kubota, "Subadaptive piecewise linear quantization for speech signal (64 kbit/s) compression," *IEEE Transactions on Speech and Audio Processing*, vol. 4, no. 5, pp. 379–382, 1996.

[20] M. Zhang, P. Shi, L. Ma, J. Cai, and H. Su, "Quantized feedback control of fuzzy Markov jump systems," *IEEE Transactions on Cybernetics*, vol. 49, no. 9, pp. 3375–3384, 2019.

[21] J. Cheng, Y. Wu, Z.-G. Wu, and H. Yan, "Nonstationary filtering for fuzzy Markov switching affine systems with quantization effects and deception attacks," *IEEE Transactions on Systems, Man, and Cybernetics: Systems*, pp. 1–10. in press, 2022.

[22] J. Yan, Y. Xia, X. Wang, and L. Li, "Quantized stabilization of continuous-time switched systems with delay and disturbance," *IEEE Transactions on Systems, Man, and Cybernetics: Systems*, vol. 52, no. 7, pp. 4530–4543, 2022.

[23] J. Cheng, Y. Wu, H. Yan, Z. G. Wu, and K. Shi, "Protocol-based filtering for fuzzy Markov affine systems with switching chain," *Automatica*, vol. 141, p. 110321, 2022.

[24] A. Kazemy and M. Hajatipour, "Event-triggered load frequency control of Markovian jump interconnected power systems under denial-of-service attacks," *International Journal of Electrical Power & Energy Systems*, vol. 133, Article ID 107250, 2021.